Variational Quantum Eigensolver applied to an Axial Next-Nearest Neighbour Ising model

Author: Adrián Copetudo Espinosa
*Facultat de Física, Universitat de Barcelona, Diagonal 645, 08028 Barcelona, Spain.**

Advisor: José Ignacio Latorre

Abstract: The phase diagram of the quantum Axial Next-Nearest Neighbour Ising model is studied with and without transverse field, in order to locate the maximally frustrated point. A Variational Quantum Eigensolver has been implemented for 4, 8 and 12 qubits, to compute the ground state energy of this Hamiltonian. Besides, the Solovay-Kitaev theorem is introduced in order to analyze how the error of the energy scales with the number of gates of the circuit.

I. INTRODUCTION

In 1982, Feynman stated that quantum computers would have a clear advantage over classical ones in simulations of strongly correlated matter [1]. In this kind of systems, finding the eigenvalues of quantum Hamiltonians is infeasible by exact diagonalization, as the dimension of physical systems grows exponentially with its size. An alternative proposal to do so is the Variational Quantum Eigensolver (VQE), which can be applied to quantum chemistry and all condensed-matter systems.

This variational method implemented in quantum computers has currently proven to be useful in large eigenvalues problems, common in quantum chemistry. For instance, photonic [2], [3] and superconducting [4], [5] quantum processors have already been tested to find the eigenvalues of some small molecules.

In this paper, the VQE is used to compute a good approximation of the ground state energy of a certain Hamiltonian, which is suitable for noisy intermediate-scale quantum computation [6]. On section II, we study an Ising model with antiferromagnetic interactions both at nearest neighbours (nn) and next-nearest neighbours (nnn) in a transverse field. This model has been widely studied using finite-size scaling [7], density-matrix renormalization group [8] and perturbative analysis [9]. This model and similar ones can be consulted in the review [10]. The Von Neumann entropy will be used as a figure of merit to analyze the phase diagram with and without transverse field, in order to choose the point with maximum frustration. On section III, both the quantum circuit simulation for a few qubits and the classical optimization method to obtain the ground state energy are explained. Each qubit of the circuit will be identified as a spin of the Ising model. On the last section, the VQE is applied to the maximally frustrated point, in order to get the ground state energy and study how the error of the energy scales with the number of gates (depth) of the circuit.

*Electronic address: adrian.copetudo@gmail.com

II. QUANTUM ANNNI MODEL

In this section, the quantum antiferromagnetic model known as the Axial Next-Nearest Neighbour Ising model (ANNNI model) is studied at zero temperature, focusing on its ground state. Quantum phase transitions occur at zero temperature and are driven by quantum fluctuations, from Heisenberg's uncertainty principle. These fluctuations are yielded by non-commuting terms in the Hamiltonian, which generate a superposition between various states, thus the system can access the different phases [10].

The main particularity of this model is that leads to frustration, which means that the system cannot have each bond in the lowest energy state. One way to obtain frustration is by using nearest-neighbours antiferromagnetic interactions in a 2-D triangular lattice. When two spins, located on the vertexes of a triangle, choose opposite orientations, the third one cannot reduce the energy of the system whatever its orientation is. However, in a few spin systems, the effects of frustration in a triangular lattice are hardly observable. A greater number of spins (and qubits) is required, but time consumption for simulations in classical computers grows exponentially with the number of qubits.

For a small number of spins, more appropriate systems that can be frustrated are antiferromagnetic Ising models with competing nearest-neighbours (nn) and next-nearest-neighbours (nnn) interactions, on a one-dimensional chain of spins. Henceforth, in one dimension for spin-$\frac{1}{2}$ fermions, using periodic boundary conditions, the Hamiltonian is defined as

$$H = J_1 \sum_{i=0}^{n-1} \sigma_i^x \sigma_{i+1}^x + J_2 \sum_{i=0}^{n-1} \sigma_i^x \sigma_{i+2}^x + \lambda \sum_{i=0}^{n-1} \sigma_i^z. \quad (1)$$

Here σ_i^x and σ_i^z are Pauli operators, J_1, J_2 and λ have dimensions of energy and n is the total number of spins.

The first term represents a ferromagnetic ($J_1 < 0$) or antiferromagnetic ($J_1 > 0$) interaction between nearest neighbours. The second term also represents a ferromagnetic ($J_2 < 0$) or antiferromagnetic ($J_2 > 0$) interaction between next-nearest neighbours. Choosing $J_1 > 0$ and the right value for J_2, frustration will be maximized. The

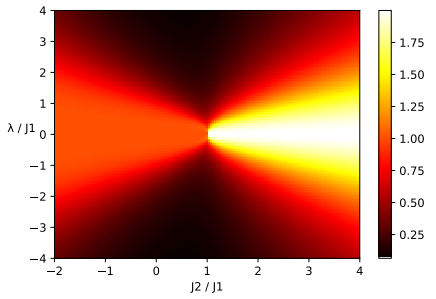

FIG. 1: Half-chain entropy with respect to $\frac{J_2}{J_1}$ and $\frac{\lambda}{J_1}$ for a 4-qubit 1-D chain. At constant $\lambda = 0$ the phase transition is located at $J_2 = J_1$, where there is a sudden growth of the entropy.

third term is due to a transverse external field of strength λ. As this term does not commute with the interaction Hamiltonian, it introduces the quantum fluctuations that enable the system to be found in any configuration with a finite probability.

Each spin can be placed either $|{\rightarrow}\rangle = |+\rangle$ or $|{\leftarrow}\rangle = |-\rangle$. On section III, these spin orientations will be interpreted as the qubit states $|0\rangle$ and $|1\rangle$, respectively. Each element of the basis of the wave function will be a classical configuration of the spins.

A. Von Neumann Entropy

The Von Neumann entropy has been used to locate where the phase transition takes place, as it is an appropriate figure of merit to measure the correlations of a system.

With n spins, or qubits, the Hilbert space is 2^n-dimensional, so we can define two subsystems of $\frac{n}{2}$ qubits, which are the two halves of the chain. Hence, $\mathcal{H} = \mathcal{H}_{n/2} \otimes \mathcal{H}_{n/2}$. The Von Neumann entropy is a dimensionless quantity that quantifies the entanglement between the two halves of the chain.

Given the ground state of the Hamiltonian, $|\psi\rangle$, and its density matrix $\rho = |\psi\rangle \langle\psi|$, the Von Neumann entropy is defined as $S(\rho) = -Tr\left(\rho \log_2(\rho)\right)$. To compute the entropy for one half of the chain, we ought to do partial traces over half of the spins to get the reduced density matrix $\rho_{n/2} = \mathrm{Tr}_{n/2}(\rho)$ and hence,

$$S(\rho_{n/2}) = -\operatorname{Tr}\left(\rho_{n/2} \log_2(\rho_{n/2})\right). \tag{2}$$

B. Entropy simulations

Using Eq. (1) with $J_1 > 0$, the entropy of half of the chain, Eq. (2), as a function of $\frac{J_2}{J_1}$ and $\frac{\lambda}{J_1}$, can be seen in Fig. (1). At constant $\lambda \to 0^+$, for $J_1 > 0$ (antiferromagnetic at nn) and $J_2 < J_1$ (both nnn ferromagnetic $J_2 < 0$ and nnn antiferromagnetic $J_2 > 0$), the 4-spin system is in a superposition of the two nn antiferromagnetic states, $|+-+-\rangle$ and $|-+-+\rangle$, with equal probability $\frac{1}{2}$. Then, the half-chain entropy is $S(\rho_2) = 2\left(-\frac{1}{2}\log_2(\frac{1}{2})\right) = 1$. However, for $J_2 > J_1 > 0$, both nn and nnn interactions are antiferromagnetic, thus the system is in a superposition of the 4 antiphase states [11], $|+--+\rangle$, $|++--\rangle$, $|-+-+\rangle$ and $|--++\rangle$, with equal probability. Therefore, the half-chain entropy is $S(\rho_2) = 4\left(-\frac{1}{4}\log_2(\frac{1}{4})\right) = 2$.

In a physical system with a finite number of spins n, a maximum of the entropy is expected at the phase transition, where the system suffers from frustration. Frustration manifests a growth of the entanglement between the two halves of the chain, but in Fig. (1) only a discontinuity can be observed. This is because, in a physical system, an spontaneous breaking of the symmetry occurs. Then, in each phase, the system chooses one of the possible states of the superposition. To model this behaviour in the simulations, an explicit symmetry breaking term, $+\epsilon(\sigma_0^x - \sigma_1^x)$, has been added to the ANNNI model of Eq. (1), where $\epsilon > 0$ has dimensions of energy and acts as a small perturbation. The strength of the perturbation must be tuned correctly to reach the product state limits, without destroying the peak of the entropy at the maximally frustrated point.

C. No transverse field

Without any transverse field ($\lambda \to 0^+$), the phase diagram shows two well-differentiated regions. When the nearest-neighbour interactions are stronger, $|J_2| < J_1$, the system behaves antiferromagnetically. Thus, the 4-spin system tends to be in a superposition of the two antiferromagnetic states. The $+\sigma_0^x$ term of the perturbation breaks the symmetry in favour of the state $|-+-+\rangle$, therefore the entropy falls to zero, as it is a product state.

However, when $|J_1| < J_2$, nnn interactions predominate and the system tends to be in a superposition of the 4 antiphase states. Due to both terms $+\sigma_0^x - \sigma_1^x$ of the perturbation, the system chooses the product state $|-++-\rangle$, with zero entropy.

In between these two behaviours, the system experiences a zero-temperature quantum phase transition at $J_2 = J_1 > 0$ (for 4 spins). At this point, frustration appears: the spins do not know how to orientate themselves and the phase transition is characterized by an increase of the entropy, which diverges as the number of spins tends to infinite [10].

When $\lambda \to 0^+$, the exact value at which the energy of both phases are equal can be computed, using Eq. (1), for a different number of spins. These transition values are $J_2 = J_1$ for 4 spins and $J_2 = \frac{J_1}{2}$ for 8 and 12 spins. The entropy simulations can be observed in Fig. (2).

Notice that as the number of spins increase, the perturbation ϵ needed to break the symmetry of the system becomes smaller. We can expect that in the thermodynamic limit $n \to \infty$, an spontaneous symmetry breaking

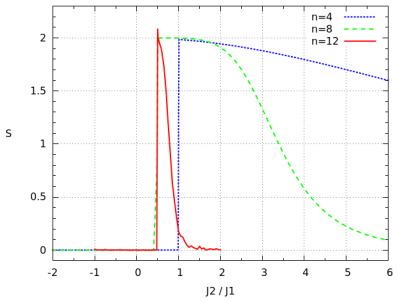

FIG. 2: Exact simulation of the half-chain entropy with respect to J_2/J_1 for different numbers of spins. A sufficiently small term $\lambda \to 0^+$ has been chosen to avoid the numerical errors related to the degeneracy of the ground state. For 4 spins (with $\epsilon/J_1 = 10^{-5}$) the phase transition occurs at $J_2/J_1 = 1$ and both for 8 spins (with $\epsilon/J_1 = 10^{-10}$) and 12 spins (with $\epsilon/J_1 = 10^{-12}$), the transition occurs at $J_2/J_1 = \frac{1}{2}$. Notice that the entropy tends to zero at both limits, as $|J_2| \to \infty$.

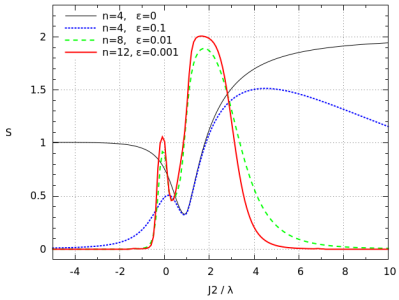

FIG. 3: Exact simulation of the half-chain entropy with $J_1/\lambda = 1$ with respect to J_2/λ in a 1-D chain for different number of spins. For very small perturbations the degeneracy is not broken, whereas for big perturbations the entropy does not reach its maximum value.

occurs without any explicit perturbation.

D. Transverse field applied

When $\lambda \neq 0$, quantum fluctuations due to the transverse field destroy the order of the system at the fully frustrated point and there is not any sudden jump of the entropy [11]. At the limits $J_2 << 0$ and $J_2 >> 0$ without any symmetry breaking term, the respective expected values for the entropy, $S \to 1$ and $S \to 2$, are recovered, as can be seen in Fig. (3).

With a transverse field $\lambda > 0$ and a sufficiently small perturbation ϵ, the Von Neuman entropy can be computed as a function of $\frac{J_1}{\lambda}$ and $\frac{J_2}{\lambda}$, so as to interpret this plot as the quantum phase diagram, Fig. (4).

For $J_1 < 0$ and $J_2 < J_1$, the system is in the ferromagnetic (FM) phase. As the ground state is two-degenerated (all spins + or all -), the explicit perturbation ϵ does not affect the system and the entropy is $S = 1$. For $J_1 > 0$ and $J_2 < J_1$, the system is in

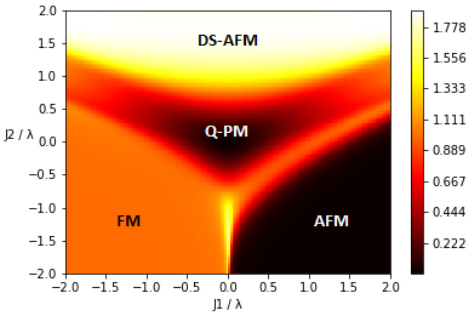

FIG. 4: Quantum J1-J2 phase diagram of the 1-D ANNNI model in a transverse field, for 8 spins. The value of ϵ has been chosen sufficiently small to distinguish the 4 phases. The entropy of the antiphase drops to zero at larger J_2/λ.

the antiferromagnetic phase (AFM). Due to the explicit perturbation, only one of the two possible antiferromagnetic product states is chosen and the entropy is zero. The above ordered region is the antiphase, also known as double-staggered antiferromagnetic phase (DS-AFM) [12]. Due to the perturbation, its entropy falls to zero at larger $\frac{J_2}{\lambda}$, as can be seen in Fig. (3). Due to the transverse field applied, in the middle of Fig. (4) lies a disordered quantum paramagnetic region (Q-PM) without any favoured state, where the spin-spin correlation function rapidly decays to zero in an open chain of spins [12]. As in the previous section, fixing $\frac{J_1}{\lambda} = 1$ two order-disorder phase transitions can be observed in Fig. (3). The absolute maximum corresponds to the Q-PM/DS-AFM transition, while the secondary maximum around $\frac{J_2}{\lambda} \approx 0$ is the AFM/Q-PM phase transition.

Comparing both quantum phase transitions, with and without transverse field, of Fig. (2) and Fig. (3), the maximally frustrated point is located without any transverse field at $\frac{J_2}{J_1} = 1$ (4 spins) and $\frac{J_2}{J_1} = \frac{1}{2}$ (8 and 12 spins).

III. VARIATIONAL QUANTUM EIGENSOLVER

Once the maximally frustrated point of the ANNNI model is located, the Variational Quantum Eigensolver (VQE) can be tested. The VQE is a hybrid classical-quantum algorithm used to find a good approximation to the ground state energy of a certain Hamiltonian H. It is based in a quantum circuit and a classical optimization method.

A. Quantum circuit

The n-qubit quantum circuit used in this paper is composed of many repeated structures called layers, which act like unitary operators upon an arbitrary initial state. Each layer is composed of rotation gates around the y-

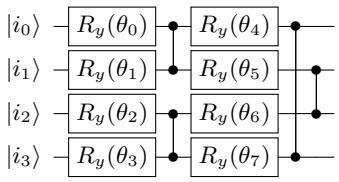

FIG. 5: Layer of a 4-qubit quantum circuit, composed by rotation and control-z gates.

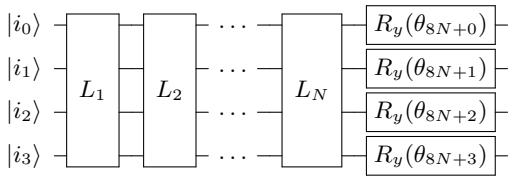

FIG. 6: Complete 4-qubit circuit composed by N layers L_i and 4 final rotation gates.

axis, $R_y(\theta_i) = e^{-i\theta_i\sigma_y}$, which act on single qubits and mix its $|0\rangle$ and $|1\rangle$ components; and control-z gates, which act on a pair of qubits and add a negative phase only if both qubits are in the state $|1\rangle$. In matrix notation both gates can be written as

$$R_y(\theta) = \begin{pmatrix} \cos\theta & -\sin\theta \\ \sin\theta & \cos\theta \end{pmatrix}, \qquad \text{C-Z} = \begin{pmatrix} 1 & 0 & 0 & 0 \\ 0 & 1 & 0 & 0 \\ 0 & 0 & 1 & 0 \\ 0 & 0 & 0 & -1 \end{pmatrix}.$$

The specific architecture of a layer can be seen in Fig. (5). It consists on n initial rotation gates, one for each qubit, $\frac{n}{2}$ control-Z gates between pairs of qubits, other n rotations and the $\frac{n}{2}$ remaining control-Z gates, connecting the remaining qubits.

The whole circuit is made by an arbitrary number of layers, N, and has n final extra rotation gates, as can be seen in Fig. (6). These last gates allow the system to choose a global phase. In total, there are $2nN + n$ rotation angles which can be tuned.

The circuit works as a unitary operator upon an arbitrary initial state, which is always chosen as the first component of the basis of n qubits, $|\psi_{\text{ini}}\rangle = |00\cdots0\rangle$, and outputs a final state $|\tilde{\psi}\rangle$, with energy

$$\tilde{E} = \frac{\langle\tilde{\psi}|H|\tilde{\psi}\rangle}{\langle\tilde{\psi}|\tilde{\psi}\rangle}. \tag{3}$$

The real physical Hamiltonian works as an unitary operator U upon an initial state $|\psi_{\text{ini}}\rangle$ to give the exact ground state $|\psi_0\rangle$. As the quantum circuit has a fixed architecture with a finite number of gates, it acts as an approximated unitary operator $\tilde{U}$. When the $2nN + n$ parameters of the circuit are tuned properly, the approximated ground state $|\tilde{\psi}_0\rangle$ can be obtained. As the variational principle states, the energy of the approximated ground state $|\tilde{\psi}_0\rangle$ will be an upper bound of the energy of the exact ground state $|\psi_0\rangle$, $\tilde{E}_0 \geq E_0$.

B. Solovay-Kitaev Theorem

The error of the approximated energy can be related to the number of layers (depth) of the circuit, by the Solovay-Kitaev theorem [13]. This theorem states that given an arbitrary unitary operator U and a desired accuracy $\mathcal{E} > 0$, there always exists an approximated unitary operator $\tilde{U}$, such that $||U - \tilde{U}|| < \mathcal{E}$. Then, this approximated operator is composed by a finite sequence of unitary gates of length $O\left(log^c(1/\mathcal{E})\right)$, where c is a constant $1 < c < 4$.

Therefore, if this arbitrary operator is taken as the Hamiltonian, it can be proven that the energy of the ground state has an error $O(\mathcal{E}^2)$, with a number of layers l that scales as

$$l \sim O\left(\log^c\left(\frac{1}{\mathcal{E}}\right)\right), \qquad \text{with} \quad 1 < c < 4. \tag{4}$$

Notice that it is an existence theorem. It is not forbidden to have a better circuit with $c < 1$. However, if a circuit has $c > 4$, the theorem states that there is always a better circuit with $1 < c < 4$.

Hence, this theorem can be used to test the quantum circuit architecture of Fig. (5), running simulations of the VQE and analyzing how the $\log\left(\frac{1}{\mathcal{E}}\right)$ scales for different numbers of layers.

C. Classical optimization

The last step before applying the VQE is choosing a classical optimization algorithm to minimize the energy of Eq. (3), adjusting the $2nN + n$ parameters iteratively. The method chosen in this paper is the gradient descent.

As the energy depends on the rotation parameters θ_i of the circuit, its variations are

$$\delta\tilde{E} = \frac{\partial\tilde{E}}{\partial\theta_i}\delta\theta_i.$$

The idea is to choose the variations of each angle in the opposite direction of the gradient of the energy, with a proportionality constant η, known as the learning ratio. The variation of the angles and the energy turns out to be

$$\delta\theta_i = -\eta\frac{\partial\tilde{E}}{\partial\theta_i}, \qquad \delta\tilde{E} = -\eta\left(\frac{\partial\tilde{E}}{\partial\theta_i}\right)^2 < 0.$$

Thus, starting at random initial angles, so as to explore the whole phase space, in each iteration of the circuit, each angle is redefined according to $\delta\theta_i$ and the energy decreases until a minimum constant value is reached. The more layers the circuit contains, the more parameters can be tuned and the closer the energy will be to the ground state. But more layers demand larger simulation times.

The main difficulty of these gradient descent methods is to appropriately vary the learning ratio to eventually reach the absolute minimum of the energy, without getting stuck in the relative ones.

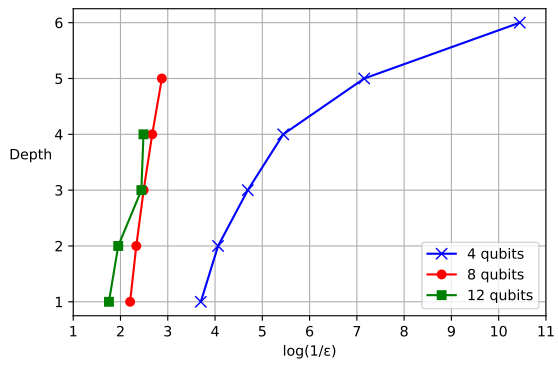

FIG. 7: Scaling of the error of the energy with the number of layers (depth) of the circuit. For n=12 qubits an scipy optimization method based on deeper gradient has been used.

IV. ANNNI GROUND STATE ENERGY

In this final section, the VQE will be used to obtain the ground state energy of the ANNNI model at the maximally frustrated point. Hence, with $\lambda \to 0^+$, so as to avoid the Q-PM phase, $\frac{J_2}{J_1}$ is chosen at the maximally frustrated point of Fig. (2): $\frac{J_2}{J_1} = 1$ for n=4, and $\frac{J_2}{J_1} = \frac{1}{2}$ for n=8 and n=12.

The Hamiltonian has dimensions of $2^n \times 2^n$. Hence, for a small number of spins, the exact ground state energy can be computed by exact diagonalization, in order to compare it with the energy obtained with the VQE. The claim is that if the VQE succeeds in finding the ground state energy (simulated in a classical computer) for a few qubits, the VQE implemented on a quantum computer is expected to succeed also for a larger number of qubits.

In Fig. (7) is shown how the logarithm of the inverse error of the energy scales with the depth of the circuit. For 4 qubits, the depth of the circuit scales log-logarithmically with the inverse error of the energy, thus, it works better than what the Solovay-Kitaev theorem states. For 8 qubits and 12 qubits, a linear improvement with the depth of the circuit can be observed. Due to the few points, the constant c cannot be determined, but the scaling of the error fulfil the Solovay-Kitaev theorem with $c \approx 1$.

V. CONCLUSIONS

The phase diagram of a quantum ANNNI model has been studied in two cases. Without a transverse field, there is a quantum phase transition at zero temperature between antiferromagnetic and antiphase states. Both the theoretical calculations and the simulations agree that the phase transition occur at $\frac{J_2}{J_1} = 1$ (4 spins) and $\frac{J_2}{J_1} = \frac{1}{2}$ (8 and 12 spins). When a transverse field is applied, a paramagnetic phase emerges in between those ones and the system experiences two phase transitions.

Choosing the maximally frustrated point, without transverse field, the VQE has been tested for different numbers of qubits to obtain the ground state energy. As seen in section IV, for 4 qubits, the circuit works better than the Solovay-Kitaev states, as the depth scales log-logarithmically with the inverse error. For 8 and 12 qubits, the scaling fulfils the theorem with $c \approx 1$, but the constant c cannot be determined with so few points.

The main difficulty of these optimization methods is to avoid falling on relative minimums. It worsens because of the infinitesimal transverse field applied to avoid the numerical errors, thus the excited energies are slightly above the ground state. Therefore, the simulations have to be run several times.

Additional improvements to the VQE would consist on implementing an Adiabatic Variational Quantum Eigensolver (AVQE), which uses a two-term Hamiltonian composed by a well-known ground state and the desired Hamiltonian, slowly evolving from one to the other.

Acknowledgments

I would like to thank my advisor, Dr. José Ignacio Latorre, for his guidance and useful discussions as well as the QUANTIC team and my parents.

[1] R. P. Feynman, Int. j. theor. phys. **21**, 467 (1982).
[2] A. Peruzzo et al., Nat. commun. **5**, 4213 (2014).
[3] B. P. Lanyon et al., Nat. chem. **2**, 106 (2010).
[4] P. J. O'Malley et al., Phys. Rev. X **6**, 031007 (2016).
[5] A. Kandala et al., Nature **549**, 242 (2017).
[6] J. Preskill, Quantum **2**, 79 (2018).
[7] P. R. C. Guimaraes et al., Phys. Rev. B **66**, 064413 (2002).
[8] M. Beccaria et al., Phys. Rev. B **73**, 052402 (2006).
[9] A. K. Chandra and S. Dasgupta, Phys. Rev. E **75**, 021105 (2007).
[10] A. Dutta et al., arXiv preprint arXiv:1012.0653 (2010).
[11] P. Sen and B. Chakrabarti, Phys. Rev. B **43**, 13559 (1991).
[12] S. Jalal and B. Kumar, Phys. Rev. B **90**, 184416 (2014).
[13] C. M. Dawson and M. A. Nielsen, arXiv preprint quant-ph/0505030 (2005).